Superalloys 718, 625, 706 and Derivatives 2005 *Edited by E.A. Loria*
TMS (The Minerals, Metals & Materials Society), 2005

THE EFFECT OF COLD ROLLING ON THE CREEP BEHAVIOR OF INCONEL® ALLOY 718

C.J. Boehlert[1], D.S. Dickmann[2], and N.C. Eisinger[3]

[1] Michigan State University, East Lansing, MI
[2] Ferro Corporation, Rochester, NY
[3] Special Metals Corporation, Huntington, WV

Keywords: microstructure, creep, backstress, creep rupture

Abstract

The creep behavior of INCONEL® alloy 718 (IN 718) was investigated to identify processing-creep property relationships. The alloy was cold rolled (CR) to 0, 10, 20, 30, 40, 60, and 80% followed by annealing and aging. In addition, this alloy can be superplastically formed (IN 718SPF) to a significantly finer grain size and the corresponding microstructure and creep behavior were evaluated. The creep behavior was evaluated in the applied stress range of 300-758MPa and the temperature range of 638-670°C. Constant-load tensile-creep experiments were used to measure the values of the steady-state creep rate and the consecutive load reduction method was used to determine the values of backstress (σ_o). Creep-rupture time (T_r) and elongation-to-failure (ε_f) were also evaluated at 649°C and 758MPa. The lowest σ_o values (300MPa<σ_0<310MPa) were exhibited for the most severely CR microstructures (60%, 80%, and IN 718SPF), while the baseline 0%CR microstructure exhibited a significantly greater σ_0 value (540MPa). The greatest σ_0 values, 645 and 630MPa, were exhibited by the 20% and 30%CR conditions, respectively. The σ_o values were related to the overall creep resistance as the 20%CR condition exhibited the lowest secondary creep rates for a given applied stress (σ_a), while the samples CR to more than 40% exhibited the greatest creep rates. The values for the effective stress exponent suggested that the transition between the rate-controlling creep mechanisms was dependent on effective stresses ($\sigma_e=\sigma_a-\sigma_0$) and the transition occurred at σ_e=135MPa for a temperature of 638°C. Increased CR tended to increase T_r and ε_f, and the 30%CR condition exhibited the greatest creep rupture properties. Overall, the 20%CR and 30%CR microstructures exhibited the greatest creep strength, while the most severely CR materials exhibited the poorest creep strength.

Introduction

In order to identify processing-creep property relationships, the current work evaluated the creep behavior of IN 718 as a function of sheet processing using 10% cold-rolling increments from 0-80% followed by annealing and aging, and the tensile-creep properties were measured. The approach taken was to characterize the creep behavior within the low-stress creep regimes where diffusional creep and grain boundary sliding may be dominating the strain rate response, and in addition the creep backstress was measured as a function of the amount of CR deformation.

® INCONEL is a registered trademark of Special Metals Corporation.

The creep mechanisms that operate during elevated-temperature deformation of pure metals and solid-solution strengthened alloys have been related to the value of the stress exponent, n_a, and the apparent activation energy, Q_a, in the Dorn steady-state creep rate equation [1]:

$$\dot{\varepsilon}_{ss} = A\, D_o \exp(-Q_a/RT)\, \mu b/kT\, (\sigma_a/\mu)^{n_a} \quad (1)$$

where T is the creep temperature in degrees Kelvin, R is the gas constant, and A is often referred to as the Dorn constant, b is the Burger's vector, D_o is the pre-exponential factor, μ is the shear modulus, and k is the Boltzmann constant. However, the n_a and Q_a values measured for alloys containing dispersed second-phase particles are generally considerably greater than those observed in pure metals and solid solution strengthened alloys [2-14]. The n_a values for precipitation-hardened alloys have ranged between 5-15 [2-7] while, for dispersion-hardened alloys, including thoria dispersed Ni-20Cr(wt.%), n_a values have ranged between 9-75 [10,13,14]. The Q_a values have ranged from one to three times those of the activation energy for self diffusion [12,14,15]. These variations in the observed values of n_a and Q_a have been rationalized by introducing the concept of a backstress or threshold stress, σ_o, which is an internal stress opposing the dislocation motion. In multiphase alloys such as IN 718, which contains an austenitic FCC phase matrix (γ) and fine γ' and γ'' strengthening precipitates, the applied stress during steady-state creep deformation is opposed by a backstress resulting from the presence of these strengthening particles and a defect structure within the material [2,10,16-21]. Therefore, the creep deformation results from an effective stress ($\sigma_e=\sigma_a-\sigma_o$). As a result, the steady-state creep rate can be represented by:

$$\dot{\varepsilon}_{ss} = A^*(\sigma_a - \sigma_o)^{n_e} \quad (2)$$

where n_e is the effective stress exponent. Although traditionally used to measure the backstress during high-stress dislocation power-law creep, it has been shown that the consecutive stress reduction method can also be applied to low-stress diffusional creep for IN 718 where low n_e values are observed [16,17].

Experimental

The IN 718 sheets used in this study were processed at Special Metals Corporation, Huntington, WV. The heats were produced by vacuum induction melting followed by electroslag remelting. The material was hot worked using conventional practices and the as-processed condition included mill annealing at 1066°C for all hot-rolling procedures which preceded the final CR and 982°C anneal. Subsequent thermomechanical processing treatments included CR between 10-80%. The CR steps were performed on separate sheets each designated with 10%, 20%, 30%, 40,%, 60%, and 80% deformation. The annealing treatment was performed at 954, 1010, or 1050°C. In addition, one set of CR samples was heat treated below the recrystallization temperature at 871°C. The aging treatment, used to precipitate out the γ' and γ'' strengthening phases, consisted of 718˚C/8h/furnace cool to 621˚C then hold at 621˚C for a total aging time of 18h. In addition, a separate heat of IN 718SPF was produced in a similar fashion, however the sheet cold working procedure, estimated to total between 55-80% deformation, was altered to assure the production of an ultrafine grain size product [22-25].

Flat dogbone-shaped tensile-creep specimens, with a cross-section of approximately 1mmx12mm and a gage length of 25mm, were machined, using either a mill or an electrodischarge machine, with the tensile axis parallel to the rolling direction. Constant-load creep experiments were performed on an Applied Test Systems, Incorporated (ATS) lever-arm

creep apparatus, using a 20:1 load ratio, in air at temperatures ranging between 638-670°C and applied stresses ranging between 300-758MPa. The creep strain was monitored during the tests using a linear variable differential transformer attached to the gage section. The specimen temperature, monitored by three thermocouples located within the gage section during the creep experiments, was maintained within ±3°C using a single-zone ATS furnace. The σ_o values were determined at 638°C by the consecutive stress reduction method [2,5,9]. When the creep rate for a given σ_a remained constant for at least five hours, it was assumed the steady-state creep rate had been achieved. Thereafter, the sample was subjected to a small stress reduction (approximately 5% σ_a). This resulted in an elastic contraction of the sample, followed by an incubation period with a zero creep rate. After a period of time, creep began again at a lower rate. Once steady state was reached, another stress reduction was performed. The time of the incubation period following each stress reduction was recorded. The remaining stress vs. the cumulative incubation time was plotted, and σ_o was determined by taking the asymptotic value of the remaining stress when the cumulative incubation time appeared to be infinite. The σ_o and $\dot{\varepsilon}_{ss}$ values proved to be repeatable as duplicate samples were tested at the same temperature and σ_a and the measured ε_{ss} values were within five percent of each other. In addition, the σ_o and ε_{ss} values were not dependent on strain history for total creep strains less than 0.5% as several temperature/applied stress conditions were performed, some in duplicate, before that of the backstress condition and in each case similar σ_o values were recorded. Creep rupture experiments were performed in air at 758MPa and 649°C. All the creep experiments were initiated after soaking the samples at the desired testing temperature for a minimum of 0.5 hours to equilibrate the thermal stresses.

Results

Microstructure

The chemical composition range of the IN 718 heats used is shown in Table I. The annealed microstructures contained an equiaxed γ-phase austenitic matrix and after aging fine γ' (coherent spherical fcc (L_{12})) and γ'' (coherent ordered disc-shaped body-centered tetragonal (DO_{22})) precipitated throughout, see Figure 1. The average γ grain diameter for the 0-40% CR sheets ranged between 16-20μm as measured through the line-intercept method. Thus 0-40% CR did not drastically change the equiaxed γ grain size. However, the 60%CR, 80%CR, and IN 718SPF microstructures exhibited an average grain diameter of 6.6μm. Annealing temperature had a significant effect on grain size. Above 1010°C, grain growth occurs [26] and the 1050°C, one-hour annealed samples exhibited a grain diameter of 45μm. It is noteworthy that the room-temperature strength and hardness values significantly increased with CR deformation for the 871°C heat-treated samples, while hardness remained almost constant after 954°C annealing. This indicated that 871°C is below the austenite (γ-phase) recrystallization temperature for 0-40%CR IN 718, which is consistent with previous findings [27]. The relatively constant hardness values for the 954°C annealed samples indicated that the annealing temperature was above the recrystallization temperature.

Table I. Composition range for the IN 718 heats used in this study

Element	Ni	Ti	Mo	Co	Cr	Al	P
Weight percent	53.68-53.48	1.01-1.06	2.99	0.03-0.12	18.1-18.4	0.46-0.48	0.009-0.012
Element	C	Fe	Cu	Si	Mn	Nb	S
Weight percent	0.03	17.99-18.3	0.02-0.17	0.01-0.17	0.04-0.12	5.07- 5.11	0.001

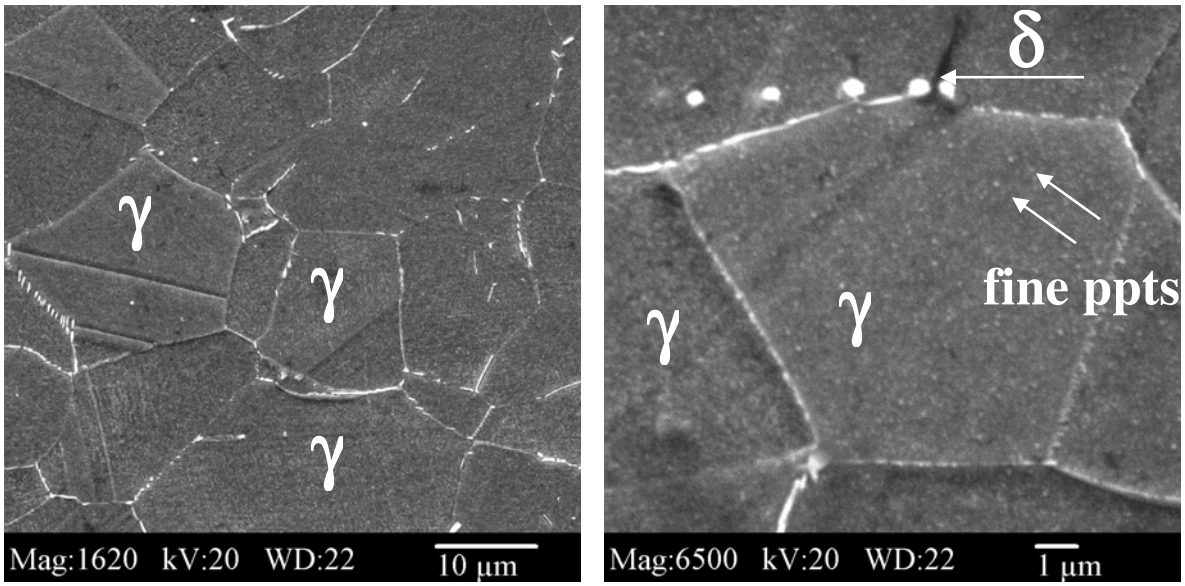

(a) (b)

Figure 1. (a) Low-magnification and (b) high-magnification SEM photomicrographs of the cross-section of a 0% cold rolled then 954°C annealed-then-aged microstructure illustrating the austenitic γ-phase matrix, fine γ' and γ'' precipitates, and δ-phase precipitates (white).

Creep Behavior

During the creep experiments the material exhibited normal creep behavior, and the strain-time plots illustrated the three stages of creep: primary, secondary, and tertiary. The dependence of $\dot{\varepsilon}_{ss}$ on σ_a is illustrated in Figure 2. The n_a values, calculated from the slopes of these curves and listed in Table II, were similar to those observed previously for IN 718 by Han and Chaturvedi [17], whose data were interpolated to 638°C and included in Figure 2 and Table II. Their data was for an as-processed condition, and it closely resembled the 0%CR data in the current work. Note that the n_a values, which ranged between 9-40, were similar to those measured for other particle-strengthened alloy systems [2-14], and are considerably larger than those generally observed for pure metals. It is apparent that there were two clusters of data, where the highest strain rates were exhibited by the samples CR to more than 40% and lower strain rates were exhibited by the 0-40%CR samples.

Figure 3 illustrates the plot used to determine σ_o while Figure 4 illustrates the corresponding $\dot{\varepsilon}_{ss}$ versus σ_e plot. The values of n_e, listed along with ε_{ss} and σ_o in Table II, were determined from equation 2. The 20%CR and 30%CR samples exhibited the greatest σ_o values, 645 and 630MPa, respectively, while the 60%CR, 80%CR, and IN 718SPF conditions exhibited the lowest σ_o values, which were less than half those of the highest σ_o values. Correspondingly the ε_{ss} values for a given σ_a were the lowest for the 20%CR and 30%CR materials, see Table II. For σ_e less than 135MPa, the n_e values were between one and two, while for σ_e greater than 135MPa, n_e was greater than 3.5, see Table II and Figure 4. The Q_a value (304$\pm$10kJ/mol) was determined for the 20%CR material using the ln $\dot{\varepsilon}_{ss}$ vs 1/T plot shown in Figure 5.

Table II. The 638°C Creep Data of IN 718 samples annealed at 954°C then aged

Cold Rolling Deformation,%	σ_a, MPa	σ_o, MPa	$\sigma_o - \sigma_a$, MPa	$\dot{\varepsilon}_{ss}$	n_a	n_e
0%	574	540	34	2.1E-09	10.8	1.2
	574	540	34	1.9E-09	10.8	1.2
	594	540	54	3.5E-09	10.8	1.2
	595	540	55	3.8E-09	10.8	1.2
	609	540	69	4.4E-09	10.8	1.2
	611	540	71	4.6E-09	10.8	1.2
	632	540	92	6.0E-09	10.8	1.2
	649	540	109	9.1E-09	10.8	1.2
	674	540	134	1.1E-08	10.8	1.2
10%	591	570	21	1.0E-09	18.3	1.7
	596	570	26	1.1E-09	18.3	1.7
	610	570	40	2.8E-09	18.3	1.7
	634	570	64	5.1E-09	18.3	1.7
	666	570	96	1.1E-08	18.3	1.7
	694	570	124	1.9E-08	18.3	1.7
20%	666	645	21	3.8E-09	39.8	1.7
	676	645	31	7.3E-09	39.8	1.7
	683	645	38	1.0E-08	39.8	1.7
30%	648	630	28	1.5E-09	36.0	1.7
	668	630	38	5.6E-09	36.0	1.7
	680	630	50	8.4E-09	36.0	1.7
40%	578	550	28	2.4E-09	13.7	1.5
	593	550	43	2.9E-09	13.7	1.5
	596	550	46	2.8E-09	13.7	1.5
	598	550	48	3.3E-09	13.7	1.5
	610	550	60	4.7E-09	13.7	1.5
	613	550	63	5.2E-09	13.7	1.5
	613	550	63	4.8E-09	13.7	1.5
	627	550	77	6.6E-09	13.7	1.5
60%	378	310	68	3.3E-09	4.6	1.0
	399	310	89	4.2E-09	4.6	1.0
	417	310	107	5.2E-09	4.6	1.0
	436	310	126	7.2E-09	10.4	3.6
	455	310	145	9.9E-09	10.4	3.6
	471	310	161	1.2E-08	10.4	3.6
	490	310	180	2.0E-08	10.4	3.6
	501	310	191	3.3E-08	10.4	3.6
	537	310	227	5.8E-08	10.4	3.6
	564	310	254	7.9E-08	10.4	3.6
	598	310	288	1.2E-07	10.4	3.6
	612	310	302	1.3E-07	10.4	3.6
80%	375	300	75	2.3E-09	4.5	1.1
	397	300	97	3.0E-09	4.5	1.1
	417	300	117	3.8E-09	4.5	1.1
	457	300	157	6.0E-09	10.3	3.9
	489	300	189	9.7E-09	10.3	3.9
	523	300	223	2.4E-08	10.3	3.9
Han and Chatervedi [17] interpolated to 638°C	620	524	96	5.9E-09	9.0	1.9
	673	524	149	1.2E-08	9.0	1.9
	696	524	172	1.7E-08	9.0	1.9
	720	524	196	2.3E-08	9.0	1.9
IN 718SPF	334	305	29	2.1E-09	5.3	1.1
	374	305	69	3.3E-09	5.3	1.1
	405	305	100	6.0E-09	5.3	1.1

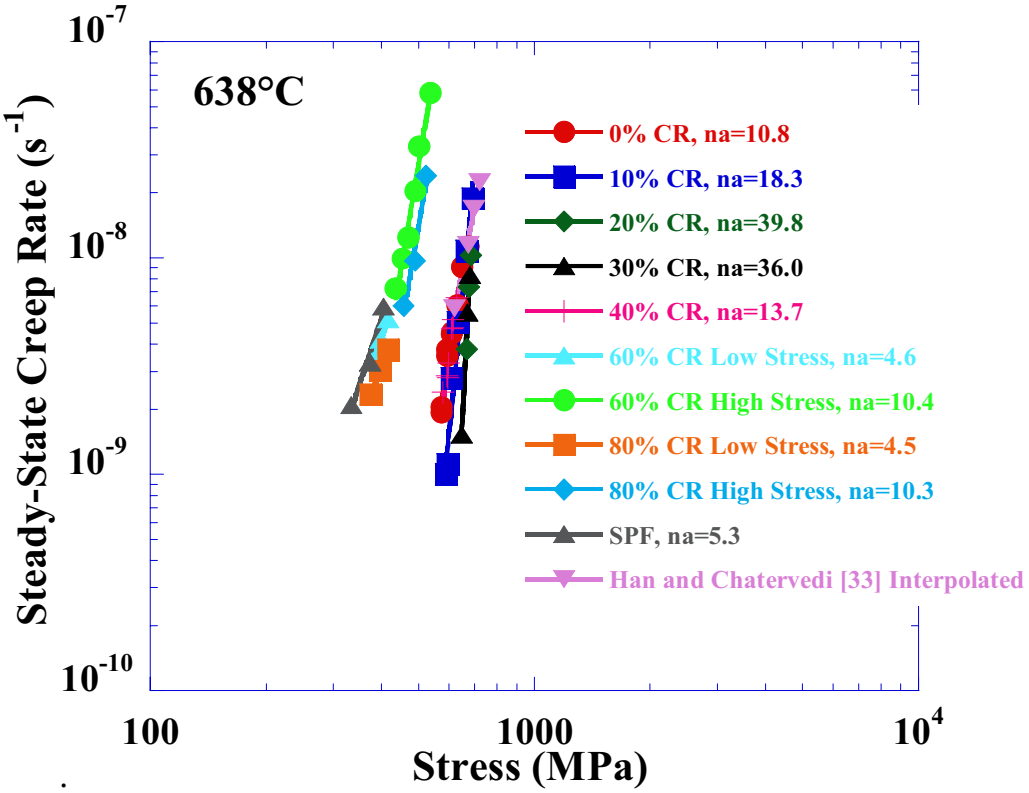

Figure 2. ε_{ss} versus σ_e plot for the 954°C annealed-then-aged IN 718 creep samples tested at 638°C. Also included is data from Han and Chaturvedi [33] which has been interpolated to 638°C.

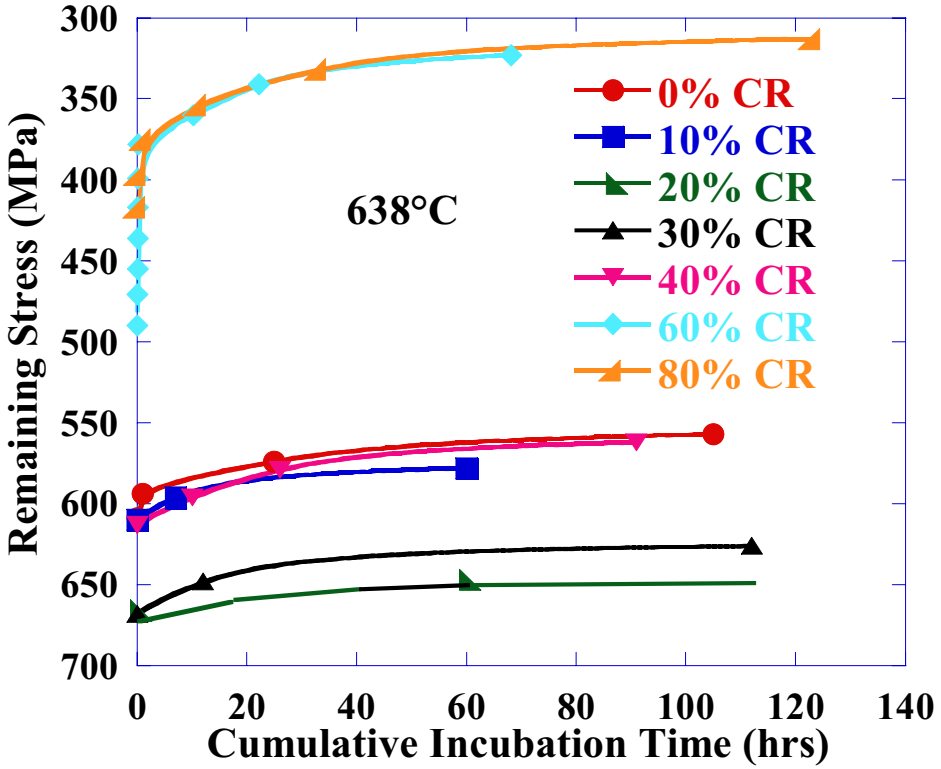

Figure 3. Remaining stress versus cumulative incubation time for the cold rolled and 954°C annealed-then-aged IN 718 creep samples.

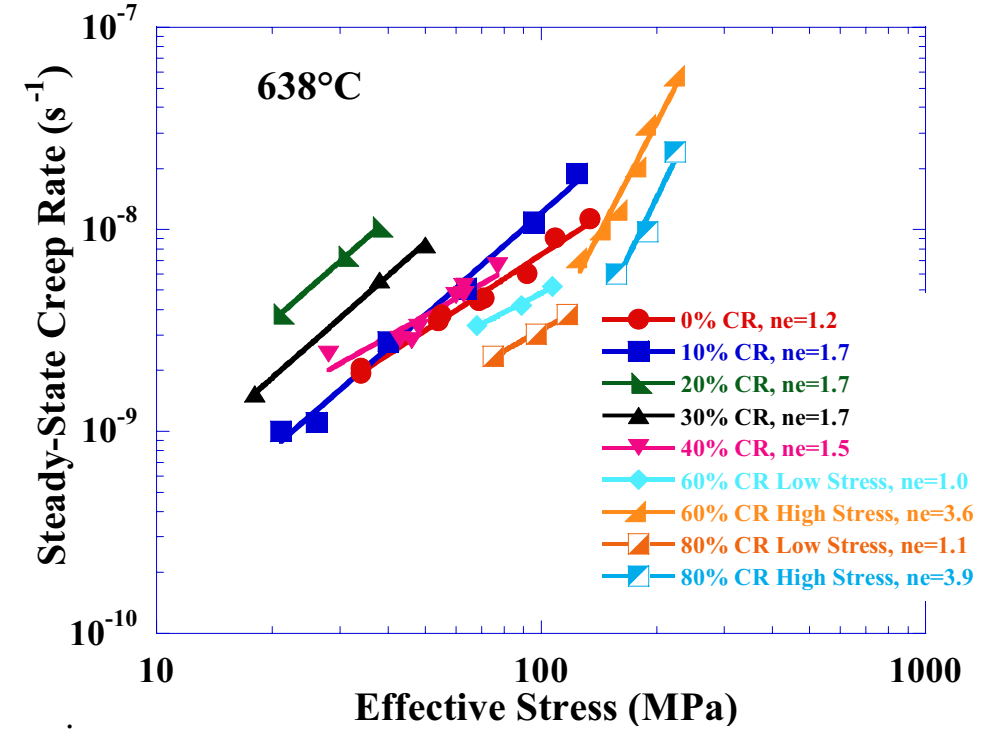

Figure 4. $\dot{\varepsilon}_{ss}$ versus σ_e plot for the cold rolled and 954°C annealed-then-aged IN 718 samples. The data was used to calculate the listed n_e values.

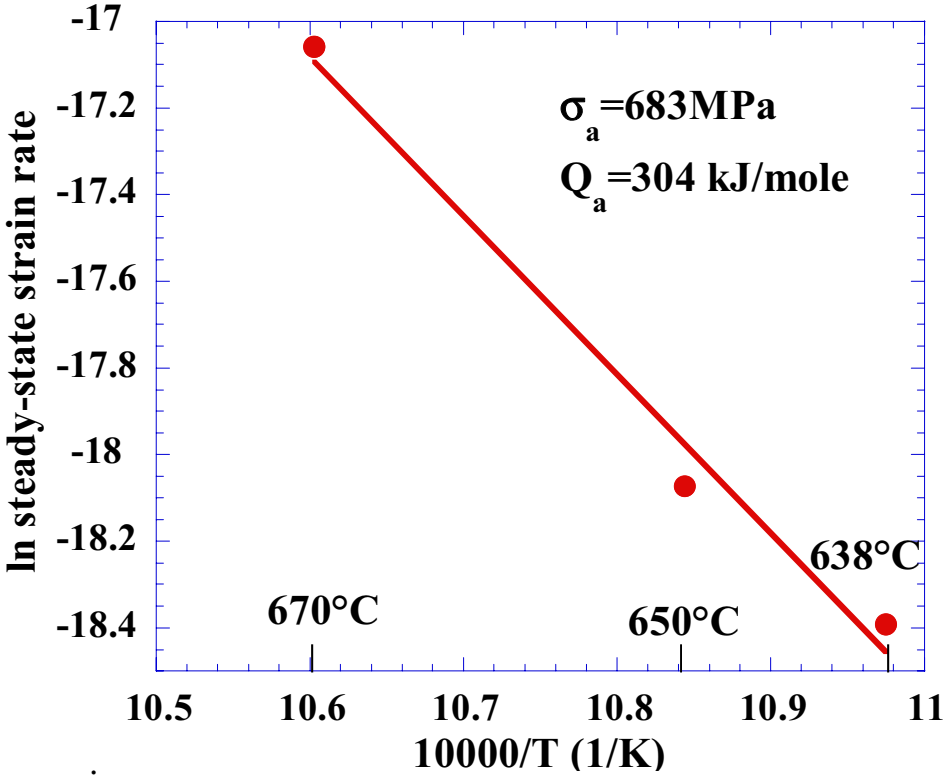

Figure 5. ln $\dot{\varepsilon}_{ss}$ vs 1/T plot used to calculate Q_a for a 20%CR 954°C annealed-then-aged sample.

The creep rupture data, listed in Table III, indicated that increased CR tended to increase T_r. For the 954°C annealed-then-aged samples, the greatest T_r and ε_f values were exhibited by the 30% and 40% cold rolled samples, where both the T_r and ε_f values were greater than twice those for the baseline 0% and 10%CR conditions. Cold rolling below 30% did not offer as significant of an increase in the creep rupture properties and both the 10% and 20%CR

conditions resulted in lower ε_f values than that for the baseline 0%CR condition. Each of the ruptured samples exhibited ductile dimpling throughout the fractured surface. The 871°C annealed-then-aged samples tended to exhibit increased T_r values with increased CR and the T_r values were significantly greater than the 954°C annealed-then-aged samples. This is considered to be a result, in part, to the greater tensile strengths exhibited by the 871°C heat-treated materials.

Table III. Creep rupture properties (649°C/758MPa) for heat-treated (*954°C,**871°C) samples

Cold Rolling Deformation, %	T_r*, hr	ε_f, * %	T_r**, hr	ε_f, ** %
0	24.9	9.3	73.6	26.1
10	27.5	6.7	65.7	25.2
20	38.5	7.9	99.8	22.0
30	64.8	28.9	103.8	18.2
40	57.9	38.0	128.9	23.8

Discussion

Creep Behavior

Effective stress exponent According to Wilshire and coworkers [2,4,5] and Gibeling and Nix [19], the consecutive stress reduction method can be used to measure σ_o during dislocation power-law creep where an incubation time after a small stress reduction is observed to occur. However, for IN 718 Han and Chaturvedi [16,17] observed an incubation time in both the power-law and the diffusional-creep regimes. According to Harris [28] and Burton [29], for diffusional creep to continue, the stress concentration at the precipitate-matrix interface created by the entrapment of diffusing vacancies can only be relieved by the formation of prismatic dislocation loops. However, Ansel and Weertman [30] have suggested that diffusional creep in two-phase alloys can only occur by the process of dislocation climb over the precipitate particles. Therefore diffusional creep in two-phase alloys may not only involve vacancy diffusion in the matrix and dislocation motion in the grain boundary region but also dislocation creation and motion within grains. Similar to the process of dislocation slip during power-law creep, dislocation climb during diffusion creep also requires dislocation networks or line segments to grow to a sufficient length so that they can be activated. These dislocation segments which become active are known as Bardeen-Herring sources [31]. Han and Chaturvedi [16] observed dislocation networks within grains where it was suggested that the observed incubation time could be due to the activation of these Bardeen-Herring sources. Therefore it was concluded that the consecutive stress reduction method can be used to determine σ_o during power-law creep as well as diffusional-creep.

The experimental results of the current work indicate two separate regimes based on the effective stress level. The n_e values were measured to be between one and two for σ_e less than 135MPa, and n_e was 3.6-3.9 for σ_e greater than 135MPa. Based on this result, the creep mechanism may be dependent on σ_e, and the low-stress regime (σ_a<450MPa) may be dominated by diffusional creep or grain boundary sliding. The mechanism of diffusional creep in particle-strengthened alloys is different from that of single-phase alloys or pure metals. Diffusional creep in the latter is known to be the result of stress-induced diffusion or the migration of matter from grain boundaries that are in tension to those that are in compression. In contrast, in particle-strengthened alloys, diffusion of vacancies will be inhibited by the precipitate particles with an accumulation of vacancies at the precipitate-matrix interface and a resultant build-up of stress concentration. This stress concentration at the interface can be relaxed by the punching of prismatic dislocation loops in the matrix, which can annihilate themselves by the absorption of

vacancies [28,29]. Therefore, to accommodate even very limited diffusional strain, in particle-strengthened alloys, additional plastic deformation must occur around precipitates either in the grain boundary region or within grains, giving an n_e value slightly greater than 1. Furthermore, diffusional creep can involve the process of dislocation climb over the particles [30]. Ansel and Weertman [30] considered the rate controlling process to be the climb of dislocations over the precipitate particles, which also depends on the diffusion rate. However, if cross-slip is also important in the above process, the creep rate will be more sensitive to stress. Han and Chaturvedi [17] observed dislocation segments and loops within grains even under the testing conditions where they considered diffusional creep to occur. Their observations suggest that the creep is more sensitive to the applied stress in particle-strengthened alloys than to that in pure metals; i.e. the value of n_e can be slightly greater than 1. This observation is in agreement with the findings of Ansel and Weertman [30], and it may also help explain the n_e values of the current work.

Activation energy The measured Q_a value (304kJ/mol) was greater than both the activation energy for self diffusion (265-280kJ/mol) and the activation energy for the creep process (276kJ/mol) of pure Ni [32] and the creep process of Ni-Cr in solid solution (295kJ/mol) [33]. However, the creep rate expression used to calculate these values considers neither the influence of temperature on the value of G nor the concept of backstress. Using the backstress, lower activation energies than those calculated using the applied stress have been calculated [17], and such values lie within the range expected for lattice self diffusion. Thus a similar result would be expected based on the Q_a measured here, and self-diffusion is considered to be more likely than grain boundary diffusion for creep of IN 718 in the temperature range of 638-670°C

Backstress The significant drop in σ_o with increased CR deformation beyond 40% was correlated with a decreasing average grain diameter of approximately 20μm for the baseline 0%CR material to approximately 6μm for the 60%CR, 80%CR, and IN 718SPF microstructures. The σ_o values observed in the current work suggest that σ_o may be dependent on grain size. At this point, the reason for the dramatic increase in backstress for the 20%CR and 30%CR conditions is not apparent and observations of the deformed samples are necessary.

Creep rupture Increased CR tended to increase T_r and ε_f. The IN 718SPF material was not evaluated in creep in this study, but based on previous creep rupture data [22] its T_r value is expected to be similar to that exhibited by the 20%CR condition. Thus there appears to be a limit to the amount of CR deformation that will result in increased creep rupture life and ε_f. This limit appears to be near 30%CR as this condition exhibited the maximum T_r value and a decrease in T_r was observed at 40%CR for the 954°C annealed-then-aged samples. It is noted that a significant decrease in the grain size occurred with increased CR from the 40%CR condition to the IN 718SPF condition, and this may be a significant factor in the creep rupture discrepancy. Comparing the creep strain rate and rupture properties, it appears that the 30%CR condition results in the most attractive overall creep behavior.

Summary

IN 718 was processed through sequential increments of CR between 0-80% followed by annealing and aging to evaluate processing-creep property relationships. The steady-state creep rate, backstress, and creep-rupture properties were measured for 954°C annealed-then-aged samples. The greatest backstress and lowest creep rate values were exhibited by the 20% and 30%CR microstructures. The lowest backstress and greatest creep rates were exhibited by the most severely CR microstructures which exhibited the finest grain size. The effective stress

exponent values, which incorporated the backstress, suggested that the creep deformation mechanism is dependent on effective stresses (σ_e) where the transition point occurs at σ_e~135MPa. Trends in the creep rupture data indicated that both T_r and ε_f increases with increased CR. Overall, the 30%CR condition exhibited the most attractive creep properties.

Acknowledgments

This work was supported by the NSF Division of Materials Research (DMR-0134789). The authors acknowledge Gaylord Smith (SMC) and James Crum (SMC) for helpful guidance.

References

1. A.K. Mukherjee, J.E. Bird, and J.E. Dorn: *Trans. Am. Soc. Metals*, 1969, vol. 62, pp. 155-79.
2. K.R. Williams and B. Wilshire: *Met. Sci. J.*, 1973, vol. 7**,** pp. 176-9.
3. D. Sidney and B. Wilshire: *Met. Sci. J*., 1969, vol. 3, pp. 56.
4. J.D. Parker and B. Wilshire: *Met. Sci. J*., 1975, vol. 9, pp. 248.
5. P.W. Davies, G. Nelmes, K.R. Williams, and B. Wilshire: *Met. Sci. J.*, 1973, Vol. 7**,** pp 87-92.
6. W.J. Evans and G.F. Harrison: *Met. Sci. J*., 1976, vol. 10, pp. 307.
7. R. Lagneborg and B. Bergman: *Met. Sci. J*., 1976, vol. 10, pp. 20.
8. D.D. Sherby and P.M. Burke: Prog. Mater. Sci., 1967, vol. 13, pp. 325.
9. J.D. Parker and B. Wilshire: Metal Science, October 1978, pp. 453-8.
10. R. Lund and W.D. Nix: *Acta Metall*., 1976, vol. 24, pp. 469.
11. C.N. Ahlquist and W.D. Nix: Acta Metall 1971, vol. 19, pp. 373-85.
12. C.L. Meyers, J.C. Shyne, and O.D. Sherby: *Aust. Inst. Met*., 1963, vol. 8, pp. 171.
13. B.A. Wilcox and A.H. Clauer: *Trans. Metall. Soc. AIME*, 1966, vol. 236, pp. 570
14. A.H. Clauer and B.A. Wilcox: *Met. Sci. J*., 1967, vol. 1, pp. 86.
15. B.A. Wilcox and A.H. Clauer: *Met. Sci. J*., 1969, vol. 3, pp. 26.
16. Y. Han and M.C. Chaturvedi: *Mater. Sci. Eng.*, 1987, vol. 85, pp. 59–65.
17. Y. Han and M.C. Chaturvedi: *Mater. Sci. Eng.*, 1987, vol. 89, pp. 25–33.
18. W. Chen and M.C. Chaturvedi: *Materials Science and Engineering*, 1994, vol. A183, p 81-9.
19. J.C. Gibeling and W.D. Nix: *Materials Science and Engineering*, 1980, vol. 45, p.123.
20. S. Purushothman and J.K. Tien: *Acta Materialia*, 1978, vol. 26, pp. 519.
21. J.H. Hausselt and W.D. Nix: *Acta Materialia*, 1977, vol. 25, pp. 595.
22. G.D. Smith and D.H. Yates: *Proc. Advancements in Synthesis and Processes*, 1992, Society for the Advancement of Material and Process Engineering, Covina, CA, pp. M207-M218.
23. G.D. Smith and H.L. Flower: *Proc. Superalloys 718, 625, 706 and Various Derivatives*, 1994, The Minerals, Metals and Materials Society, Warrendale, PA, pp. 355-364.
24. B.A. Baker: *INCO Alloys International Technical Investigation Report No. BAB1323093*, Huntington, WV. September 1993.
25. Y. Huang and P.L. Blackwell: *Materials Science and Technology*, 2003, Vol. 19, pp. 461-6.
26. INCONEL alloy 718 Bulletin, 4th Edition, 1985, published by The International Nickel Company, Inc., now Special Metals Corporation, p.1-25
27. W.C. Liu, Z.L. Chen, and M. Yao: *Metall. and Materials Transactions*, 1999, 30A, p 31-40.
28. J.E. Harris: *Met. Sci. J*., 1973, vol. 7, p.1.
29. B. Burton: *Materials Science and Engineering*, 1973, vol. 11, pp. 337.
30. G.S. Ansel and J. Weertman: *Trans. Metall. Soc. AIME*, 1959, vol. 215, p.838.
31. D. Hull: Introduction to Dislocations, Pergamon, Oxford, 1975, pp.188-190
32. J.P. Dennison, R.J. Llewellyn, and B. Wilshire*: J. Inst. Met*., 1967, vol. 95, p.115.
33. D. Sidey and B. Wilshire, *Met. Sci. J*., 1969, vol. 3, p.56.